Renewable and Sustainable Energy Reviews 69 (2017) 144–155

Contents lists available at ScienceDirect

Renewable and Sustainable Energy Reviews

journal homepage: www.elsevier.com/locate/rser

# Inertia response and frequency control techniques for renewable energy sources: A review

Mohammad Dreidy, H. Mokhlis*, Saad Mekhilef

*Department of Electrical Engineering, Faculty of Engineering, University of Malaya, 50603 Kuala Lumpur, Malaysia*

ARTICLE INFO

*Keywords:*
Deloading control
Energy storage system (ESS)
Frequency regulation
Inertia
Load shedding
Over-speed control
Rate of change of frequency (ROCOF)
Renewable energy source (RES)

ABSTRACT

Preservation of the environment has become the main motivation to integrate more renewable energy sources (RESs) in electrical networks. However, several technical issues are prevalent at high level RES penetration. The most important technical issue is the difficulty in achieving the frequency stability of these new systems, as they contain less generation units that provide reserve power. Moreover, new power systems have small inertia constant due to the decoupling of the RESs from the AC grid using power converters. Therefore, the RESs in normal operation cannot participate with other conventional generation sources in frequency regulation. This paper reviews several inertia and frequency control techniques proposed for variable speed wind turbines and solar PV generators. Generally, the inertia and frequency regulation techniques were divided into two main groups. The first group includes the deloading technique, which allow the RESs to keep a certain amount of reserve power, while the second group includes inertia emulation, fast power reserve, and droop techniques, which is used to release the RESs reserve power at under frequency events.

## 1. Introduction

Recently, air pollutants generated by fossil fuel power plants, such as carbon dioxide, nitrogen oxide, and Sulphur dioxide are causing serious environmental problems [1]. Acid rain and global warming are regarded as major causes of the environmental pollution [2,3]. In the United States, fossil fuel power plants emit about 2.2 billion tons of carbon dioxide ($CO_2$) annually [4]. These problems forced governments and other agencies around the world to set targets in increasing the application of RESs in the generation of electrical power [5]. China, for example, has set a target of generating over 15% of its total power from renewable energy by 2020 with 420 GW of hydro, 50 GW solar, 200 GW of wind, 30 GW of biomass. As shown in Fig. 1, several countries set different future prospective targets in increasing power generation from RESs. These plans are crucial in order to address the tremendous increase in world energy demand while simultaneously reducing the amount of pollutions.

Generally, integrated RESs in a power system decreases dependence on fossil fuel, improve voltage profile, and increase the reliability of power system [7–10]. However, the high penetration of RESs can lead to critical frequency stability challenges [11]. First, the RESs typically have low or non-existent inertial responses [12]. For example, the variable speed wind turbines are usually connected to the network by power electronic converter, which effectively decouple the wind turbine inertia from mitigating system transients. Furthermore, solar photovoltaic plants do not provide any inertia response to the power system. Therefore, replacing conventional sources with RESs will reduce the inertia of the whole power system. This fact is supported by [13,14] both of which predicted that the increasing number of RESs in the UK could reduce the inertia constant by up to 70% between 2013/14 and 2033/34. Due to this inertia reduction, the Rate of Change of Frequency (ROCOF) of the power system will be high enough to activate the load-shedding controller, even at a small magnitudes of imbalance. In [15], different penetration levels of RESs were used with a Synchronous Generator (SG) to cover 3.8 MW load demand. As reported in [15] and shown in Fig. 2, the ROCOF of the power system increase whenever the percentage-installed capacity of the RESs increases.

Second, an increase in the penetration level of the RESs decreases the number of generation units providing reserve power for primary and secondary control. For this reason, the frequency deviation will be increased, as reported in [16] and shown in Fig. 3.

To overcome the frequency stability challenges represented by small inertia response and reserve power, RESs must create new frequency control techniques to allow them to participate in frequency regulation operations. This paper presents a comprehensive review of inertia and frequency control techniques for solar PV and wind turbines. These techniques enable the RESs to increasingly stabilize the power system. This paper is organized in the following order. Section 2 will discuss the frequency response of conventional power

* Corresponding author.

http://dx.doi.org/10.1016/j.rser.2016.11.170
Received 16 November 2015; Received in revised form 18 July 2016; Accepted 12 November 2016

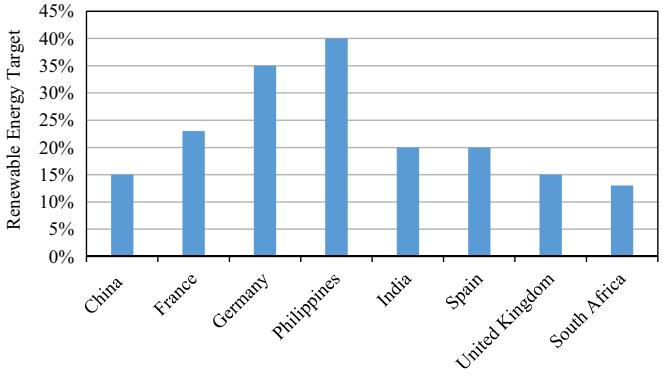


**Fig. 1.** Renewable energy targets by country for 2020 [5,6].

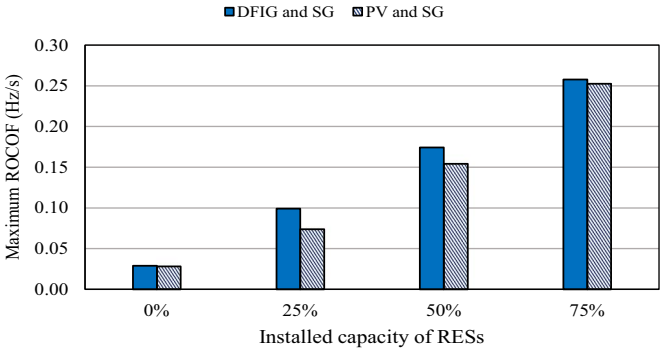


**Fig. 2.** Maximum ROCOF of the Microgrid for two types of RESs supply 3.8 MW load [15].

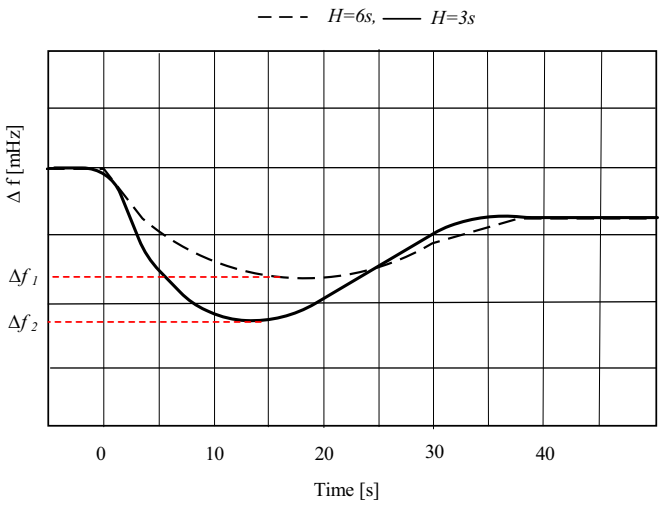


**Fig. 3.** Frequency deviation for two different inertia constants [16].

sources. Section 3 will present several inertia and frequency control techniques for RESs without ESS. Section 3.1 will present several inertia and frequency control techniques for RESs with ESS. Section 3.1.1 will explain the different soft computing approaches used with frequency regulation control. Section 3.1.1.1 will discuss the advantage and disadvantages of each control methods. The conclusions and future research will be presented in Section 3.1.1.2.

## 2. Frequency response of conventional power sources

The general frequency response with operation limits corresponding to England and Wales are shown in Fig. 4. During normal operations, the system frequency is close to 50 Hz. However, when an event occurs that causes generation-demand unbalance, the system

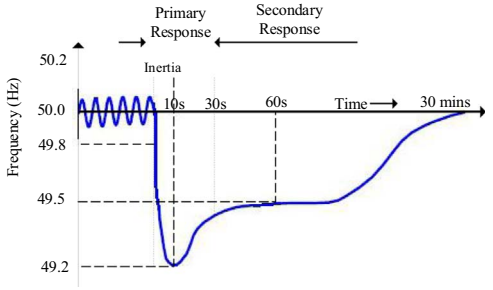


**Fig. 4.** Time frames involved in system frequency response [21].

frequency starts to decline with the frequency rates, depending on the total system inertia and the amount of unbalanced power, as given by the swing equation [17,18]:

$$\frac{df}{dt} = \frac{fo}{2H_{sys}S_B}(P_m - P_e) \quad (1)$$

where $df/dt$ is the rate of frequency change, $H_{sys}$ is the total system inertia constant, $S_B$ is the rating power of the generator, $P_m$, $P_e$ are the mechanical power and electrical power, respectively, and $f_o$ is the system frequency. Prior to any controller activation and due to inertia response, the synchronous generator releases the kinetic energy stored in its rotating mass, which lasts for ~10 s [18,19]. After that, if the frequency deviation surpasses a specific value, the primary frequency controller will be immediately activated. This controller use the generator governor to return the frequency to save values within 30 s [19,20]. After 30 s, a new control called the secondary control will be activated to return the system frequency to its nominal value.

As shown in Fig. 4, the secondary controller needs several minutes to recover the system frequency to its nominal value. Therefore, a reserve power should be available to cover the increase in power demands during this period. Finally, the remaining power deviation activates the tertiary frequency control. Differing from primary and secondary controllers, tertiary controller requires manual adjusting in the dispatching of generators or changes of the schedule periods. This paper does not deal with this type of controller [22]. Generally, Inertia and frequency control techniques for RESs is commonly divided into two main categories; control techniques for RESs without any support from ESS and control techniques for RESs with ESS. Fig. 5 illustrates the different techniques that fall under each category:

## 3. Control techniques designed for RESs without energy storage systems

In order to minimize the negative impact of high RESs penetration, different inertia and frequency control techniques for RESs with and without ESS can be considered. These techniques enable RESs, such as wind turbine and solar PV plants, to contribute to the frequency regulation.

### 3.1. Wind turbine

Wind energy is one of the most applied renewable sources throughout the world. Many countries that have wind energy potential started replacing conventional power plants with wind energy plants. Statistics show that future wind penetration in the U.S. and Europe will exceed 20% within the next two decades [23].

There are two main categories of wind turbine; fixed speed and variable speed [24]. A fixed speed wind turbine generally uses an induction generator that is connected directly to the grid and can provide an inertial response to the frequency deviation, even though this inertia is small compare to the synchronous generator. A variable speed wind turbine mainly uses a Permanent Magnet Synchronous Generator (PMSG), or DFIG. The PMSG is fully decoupled from the

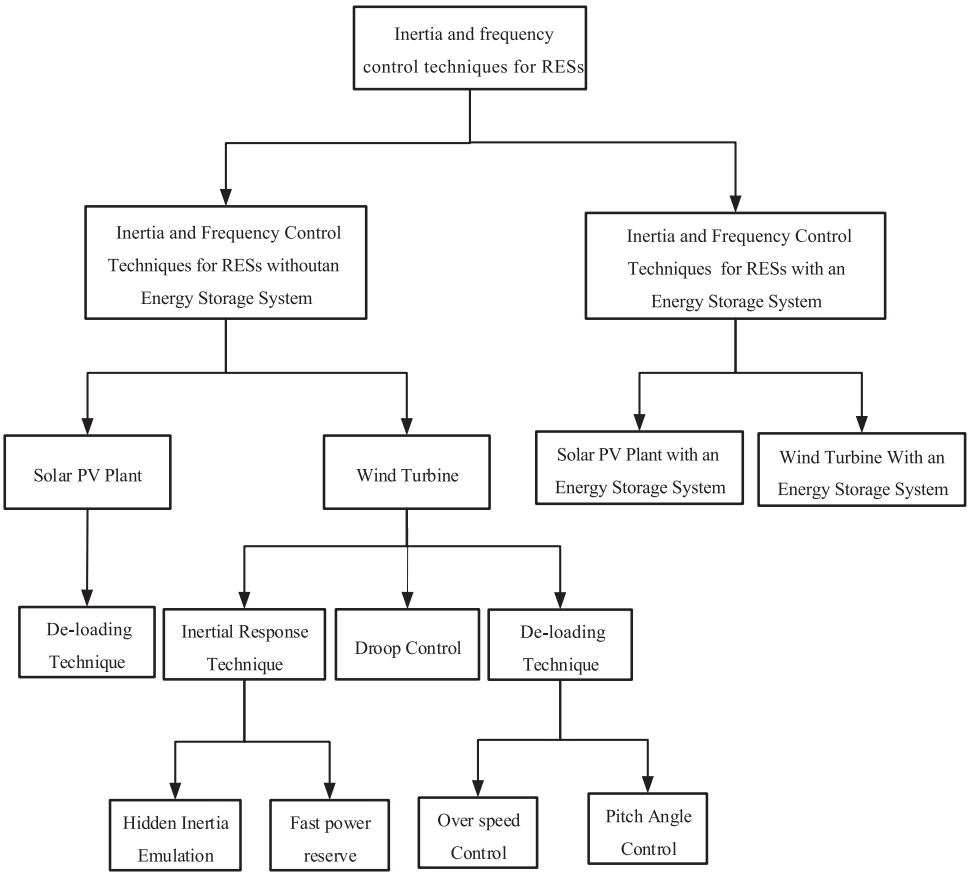


**Fig. 5.** Inertia and frequency control technique design for RESs.

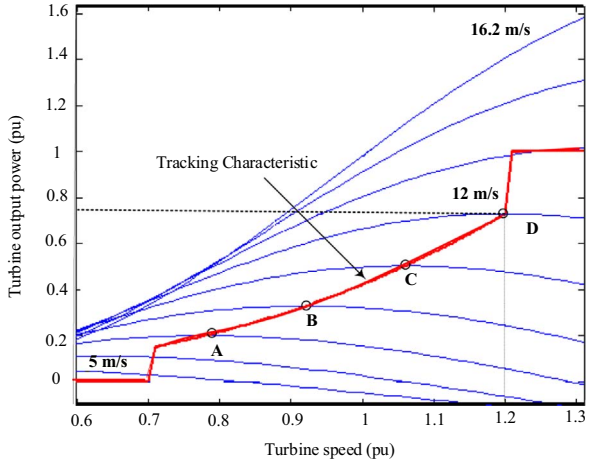


**Fig. 6.** Power against rotating speed characteristics at (Pitch angle β=0) [28].

grid; this is because the stator of this type of generator is connected to the power electronic converter in order to inject the power into the grid. The DFIG is similar to the PMSG, except for the fact that this generator is connected to the grid via a rotor circuit. The power electronic converter used in a variable speed wind turbine enables the wind turbine to regulate the output power over a wide range of wind speeds [25]. However, this coupling isolates the wind turbine from the frequency response under disturbance. Additionally, traditional wind turbines follow the maximum power plot, as shown in Fig. 6. Therefore, they do not have reserve power to support frequency control. The maximum output power from a wind turbine, defined as a function of rotor speed, is given by [26,27].

$$P_{MPPT} = K_{opt}\omega^3 \tag{2}$$

where $\omega$ is the rotor speed and $K_{opt}$ is the constant (controller gain) for the tracking of the maximum power curve, and obtained by:

$$K_{opt} = 0.5\rho\pi R^5 \frac{Cp_{opt}}{\lambda opt^3} \tag{3}$$

where $\rho$ is the air density, $R$ is the radius of the turbine wheel, $Cp_{opt}$ is the maximum power coefficient, $\lambda_{opt}$ is the optimum tip speed. The maximum power point controller determines the operating point along the power load line. This operation was conducted using the speed regulation of wind turbine within the speed limits and pitch regulation after the rated speed.

Researchers have investigated two main techniques to support frequency control using a variable speed wind turbine, inertia response, and power reserve control. Inertia control enables the wind turbine to release the kinetic energy stored in the rotating blades within 10 s to arrest the frequency deviation, while reserve control technique uses the pitch angle controller, speed controller, or a combination of the two to enhance the power reserve margin during unbalanced power events.

### 3.1.1. Inertia response control

Unlike conventional generators that can automatically release the kinetic energy stored in their rotating mass, wind turbines do not have the same ability to release the kinetic energy stored in rotating blades. For this reason, the wind turbine need a suitable controller to provide inertia response. Generally, there are two control techniques that deal with inertia response; inertia emulation and fast power reserve. Inertia emulation is the first technique; it proposes new control loops to release the kinetic energy stored in rotating blades of wind turbine. This additional power is used to terminate the frequency deviation during unbalance events. Fast power reserve is the second technique,

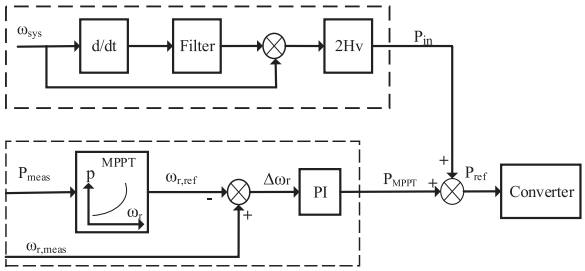


**Fig. 7.** Inertia emulation for variable speed wind turbines [30].

which can also be used to terminate the frequency deviation. However, this technique responds to frequency deviations by releasing constant power for a set amount of time.

*3.1.1.1. Inertia emulation.* Using a power electronic converter with a suitable controller enables the variable speed wind turbines to release the kinetic energy stored in their rotating blades. This kinetic energy is used as an inertia response in the range 2–6 s [29]. Generally, there are two types of inertia response; one loop inertia response and two-loop inertia response. In the former, one loop control based on the ROCOF is used to release the kinetic energy stored in the rotating blades, while the latter uses two loops based on ROCOF and frequency deviations. In [21,30–32] the one loop inertia response is added to the speed control system to enable the wind turbine to respond to the ROCOF. This control loop is called inertia emulation, which exactly emulates the inertia response of conventional power plants, as shown in Fig. 7.

The output power from wind turbine $P_{meas}$ determine the reference rotor speed $\omega_{r,\ ref}$, which is compared to the measuring rotor speed $\omega_{r,\ meas}$, and used by the PI controller to provide maximum power. During normal operations, the reference power transferred to the converter is equal to the maximum power without any contribution from the inertia control loop. After a power deficit, a certain amount of power $P_{in}$ based on the value of ROCOF and virtual inertia constant $H_v$ will added to the $P_{MPPT}$. Due to the power increment, the generator will slow down, and the kinetic energy stored in the rotating wind turbine blades will be released. The additional power Pin comes from the inertia response loop, which depends on ROCOF, and is given by [33]:

$$P_{in} = 2H_v \times \omega_{sys} \times \frac{d\omega_{sys}}{dt} \tag{4}$$

Due to the constant additional power resulting from the inertial control loop, this type of control has two disadvantages. First, the rotor speed is rapidly reduced, leading to big losses in aerodynamic power. Second, the controller takes time to bring back the energy during rotor speed recovery. These disadvantages can be avoided, as per [34], where a new inertia response constant is formulated. This constant is called the effective inertia response, which is based on frequency value. Generally, the inertia constant for a wind turbine is defined by:

$$H = \frac{E_{kin}}{S_B} = \frac{J\omega^2}{2S_B} \tag{5}$$

where $E_{kin}$ is the kinetic energy stored in the rotating mass of the wind turbine, SB is the rated power, and J is the moment of inertia. Eq. (5) can be rewritten by substituting the corresponding power from Eq. (2). Then, the effective inertia constant will be:

$$He(\omega) = \frac{J\lambda^3 opt}{\rho\pi R^5 C_p opt}\frac{1}{\omega} \tag{6}$$

The main idea is to increase the value of the inertia constant as long as the system frequency continues to decline. Consequently, the torque transfer to the converter is reduced, as shown in Fig. 8.

The principle of the one loop inertia response discussed earlier is

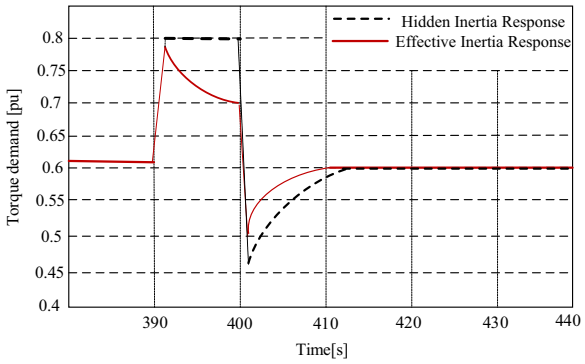


**Fig. 8.** Torque demand due to inertia response [34].

that it provides a decelerating torque signal proportional to ROCOF. This decelerating torque lasts until frequency is restored. Consequently, without support from another controller, the overall reference torque injected into the converter $T_{elec}^{*}$ will be decreased by the maximum power point, which is working to bring back the system to the optimum curve. As a result, the power injected into the grid will be reduced directly and bring back the frequency support immediately. In order to avoid this re-acceleration of wind turbine, [35,18][18,35] proposed a two loop control inertia response, as shown in Fig. 9. This control provides an additional torque $\Delta T$, which is proportional to frequency deviation and lasts until nominal frequency is recovered. The two loop inertia response control system with two additional modifications is presented in [36]. A new block called delay speed recovery is added to recover the turbine speed as soon as possible. A wave filter is the other modification, which is adapted in the $\Delta f$ loop to avoid constant value. In this paper, the author also discusses the effect of different values of $K_1$ and $K_2$ on system stability.

*3.1.1.2. Fast power reserve.* Generally, the inertia response can be emulated, as the control signal depends on the frequency deviation or ROCOF, as pointed out previously. It can also be defined as a constant 10% of the nominal active power for 10 s, despite various wind speeds [37]. The short-term constant power, which is called the fast power reserve, is released from the kinetic energy stored in the rotating mass of the wind turbine. This fast power reserve can be achieved by controlling the rotor speed set point. This is given by:

$$P_{const}t = \frac{1}{2}J\omega ro^2 - \frac{1}{2}J\omega rt^2 \tag{7}$$

where $P_{const,}$ is the constant amount of active power, t is the time duration for the fast power reserve, $\omega_{ro}$ is the initial rotational speed, and $\omega_{rt}$ is the rotational speed at the end of inertial response. Thus, the reference rotational speed can be obtained by:

$$\omega r,\ ref = \omega rt = \sqrt{\omega ro^2 - 2\frac{Pconst}{J}t} \tag{8}$$

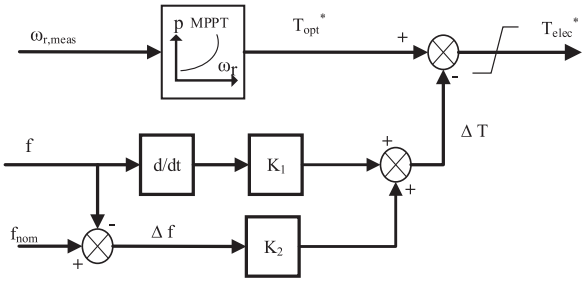


**Fig. 9.** Supplementary control loops for inertia response [35].

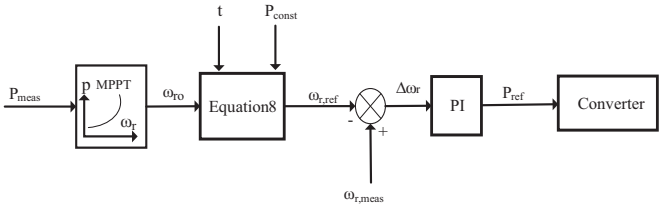


**Fig. 10.** Fast power reserve controller for a wind turbine [30].

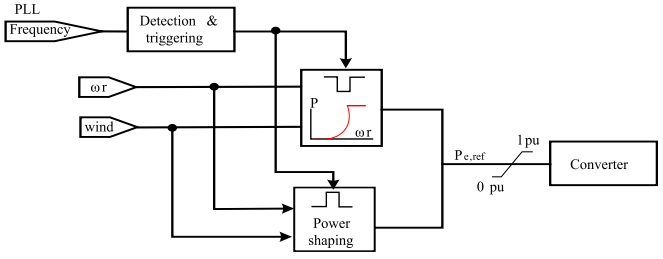


**Fig. 11.** Block diagram of fast power reserve controller.

Different works in literature have discussed the principle operation of the fast power reserve. References [38,39] discussed the capability of variable speed wind turbines to provide short term overproduction power for different wind speeds. In fact, these two papers did not provide any controller design for fast power reserve. However, [30] proposed a fast power reserve controller system for a wind turbine, as shown in Fig. 10. The amount of constant power and the time duration determines the rotor speed in accordance with Eq. (8).

Ref. [40] proposed an architecture for a fast power reserve controller, as shown in Fig. 11. This figure contains a detecting and triggering scheme, power shaping, and an MPPT controller.

The operation of the fast power reserve controller begins once the frequency deviation exceeds a certain threshold; a control signal is sent from the detecting and triggering scheme to bypass the maximum power point tracking and enables power shaping, as shown in Fig. 12. This scheme continues providing extra power during overproduction. However, when the kinetic energy discharge is complete, the speed recovery function brings the rotor speed back to its pre-event value, and restores the maximum power. This restoration often leads to the under-production phase, in which power is withdrawn from the grid to return the rotor speed to its desired value. To avoid an immediate drop in the output power, the transition from overproduction to under-production should follow a sloped transition.

Different strategies for fast power reserve for wind farms were proposed in [41]. The author discussed the operation of a centralized controller, which is responsible for frequency regulation. This central controller has two main tasks, the first task being to determine the amount of additional power for each wind turbine, while the second task is to determine the appropriate time to recover kinetic energy after over production is finished.

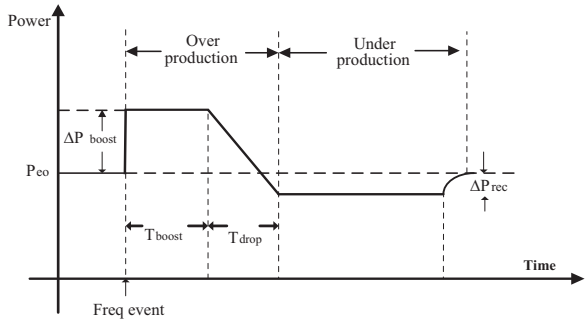


**Fig. 12.** Power characteristics for fast power reserve control [40].

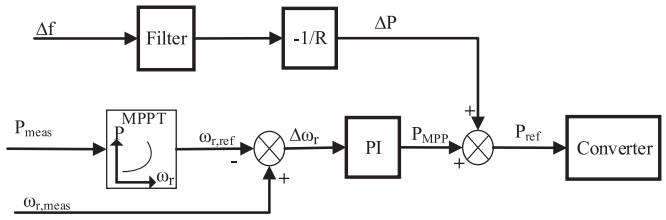


**Fig. 13.** Frequency support scheme with droop speed control [44].

### 3.1.2. Droop control

The droop control scheme shown in Fig. 13 regulate the active power output from a wind turbine proportional to frequency change. This controller greatly improves the frequency nadir as well as the frequency recovery process following disturbances. The active power is adjusted according to linear characteristics, and is given by [42–44].

$$\Delta P = P1 - Po = -\frac{f_{meas} - f_{nom}}{R} \tag{9}$$

where $R$ is the droop constant, $f_{meas}$ and $P_1$ are the new frequency and wind turbine output power, respectively, while $f_{nom}$ and $P_o$ are the initial operating points.

The linear relation between frequency and the active power of the wind turbine is illustrated in Fig. 14. When the frequency falls from $f_{nom}$ to $f_{meas}$, the wind turbine increases the output of power from $P_o$ to $P_1$ to compensate for frequency deviations [45].

### 3.1.3. Deloading control

From an economic point of view, wind turbines are designed to operate on an optimum power extraction curve. As a result, they do not participate in frequency regulation. For this reason, sufficient reserve capacity must be available in the system to address any frequency deviation. Deloading is a new technique to ensure a reserve margin by shifting the wind turbine's operating point from its optimal power extraction curve to a reduced power level. Based on the wind turbine's aerodynamic behaviour, the mechanical output power captured by the wind turbine will be:

$$P_m = \frac{1}{2}\rho A C_p(\lambda, \beta) v^3 \tag{10}$$

where $\rho$ is the air density, $A$ is the rotor sweep area, $v$ is the wind speed, $C_p$ is the power coefficient, $\beta$ is the pitch angle, and $\lambda$ is the tip speed ratio, which is given by:

$$\lambda = \frac{\omega_r R}{v} \tag{11}$$

From Eq. (10), it is clear that the output power of the wind turbine is dependent on the tip speed ratio $\lambda$ and pitch angle $\beta$. In general, the deloading technique has two types of control system; speed control and pitch angle control.

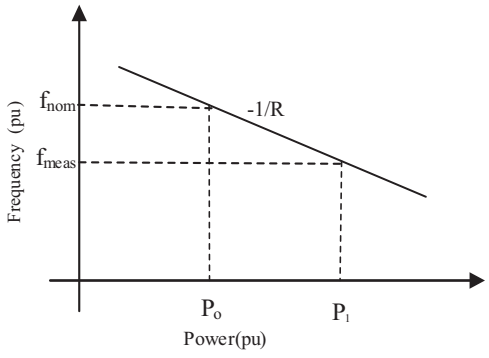


**Fig. 14.** Wind turbine droop characteristics.

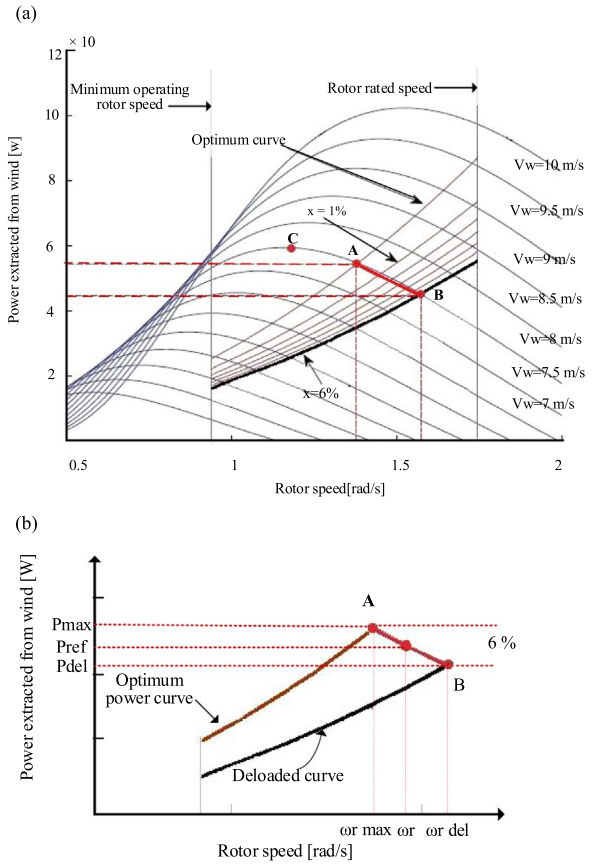


**Fig. 15.** (a) MPPT and deloaded power curves of wind turbine [46]. (b) Calculation of power reference for 6% deloaded operation [46].

*3.1.3.1. Deloading by speed control.* Speed control is suggested to change the value of the tip speed ratio $\lambda$ by shifting the operating point towards the left or the right of the maximum power point, as shown in Fig. 15 (a). This figure illustrates the deloading function of a 1.5 MW DFIG-based wind turbine by (1-x) of the maximum power under definite wind velocity ($V_W$). The wind turbine running at point A can be deloaded by the under-speed or over-speed control. For the under-speed control, the operating point of the wind turbine moves towards point C, while for the over-speed control, the operating point of the wind turbine moves towards point B, which is preferable.

Referring to Fig. 15(b), when the system frequency drops, the wind turbine releases a definite amount of active power proportional to frequency deviation. Then, the operating point will be located between A and B with $P_{ref}$, given by:

$$P_{ref} = P_{del} + (P_{\max} - P_{del}) \times \left[ \frac{\omega r_{del} - \omega_r}{\omega r_{del} - \omega r_{\max}} \right] \quad (12)$$

where $P_{max}$ is the maximum power (pu), $P_{del}$ is the deloaded power (pu), $\omega_{r\,max}$ is the rotor speed at maximum power, $\omega_{r\text{-}del}$ is the rotor speed at de-loaded power, $\omega_r$ is the rotor speed corresponding to reference power. Generally, deloading using over-speed control is preferably used at medium wind speeds.

*3.1.3.2. Deloading by pitch angle control.* Pitch angle is the second controller used to deload the wind turbine by increasing the blade's angle. It is preferred that this controller is activated when the wind turbine generator arrives at the rated speed and when the over-speed controller fails to perform this operation.

Fig. 16 shows the power-rotor speed curve for a DFIG wind turbine

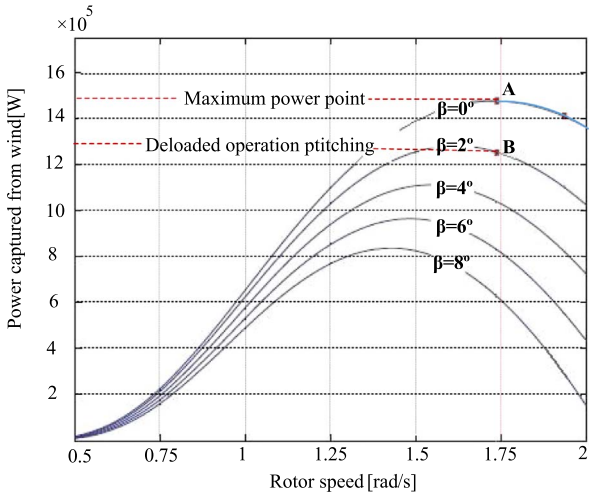


**Fig. 16.** Power rotor-speed curves for different values of pitch angle for a 1.5 MW wind turbine (wind speed: 10 m/s) [46,18][18,46].

under different pitch angles. This figure illustrates the deloading technique for a wind turbine running at point A; in this case, the controller fails to increase the rotation speed over the rated speed. Then, the pitch angle controller begins to increase the angle of the wind turbine blades and shifts the operating point from point A to point B without any change in the rotor's speed.

Generally, several different works in the literature have dealt with the deloading technique, as it is used with a variable speed wind turbine, as per [47]. The deloading technique supports primary frequency control under two operating conditions, as shown in Fig. 17. In normal conditions, the variable speed wind turbine works at the optimal power curve, extracting the operating point from the look-up table. However, when the deloading switch is turned on, the deloading mode will be activated. In this case, the speed and pitch angle controllers will cooperate to allow the wind turbine to reserve some power under different modes. Eq. (12) determines the reference power for speed and pitch control to provide a 10% reserve power. To release the active power stored in the rotating mass due to deloading control, droop control is also presented in this work. The amount of releasing power is proportional to frequency deviations, and is limited to 10% of wind turbine rated power.

[48] presents the inertia response and primary frequency for DFIG-based wind turbines. The inertia controller is emulated to release the kinetic energy stored in the wind turbine rotating blades for a few seconds. It is proposed that a deloading strategy with 90% sub-optimal power functions as the primary frequency control. This strategy, based on cooperation between the speed and pitch controllers, provides the wind turbine with relatively long-term reserve power. Fig. 18 shows the deloading technique used with a wind turbine in three operating modes. In the first operating mode, the over-speed control is used to deload the wind turbine. For example, the deloading of the wind turbine running at point F by 90% sup-optimal power was done by increasing the generator rotor speed towards point C. In the second operating mode, the over-speed and pitch angle controller were combined to achieve a certain sup-optimal power. For example, to deload the wind turbine running on point B with 90% sup-optimal power, the over-speed controller needs to shift the operating point towards point D. However, the over-speed controller increased the speed until the wind turbine arrives at point G. After that, the over-speed controller will not be able to increase the rotation speed any longer. As a result of this, the pitch angle controller increases the blade pitch angle, which shifts the operating point towards point A. In the third region, the pitch controller is used by itself to achieve the target deloading value.

The cooperation between pitch angle and speed controller for a

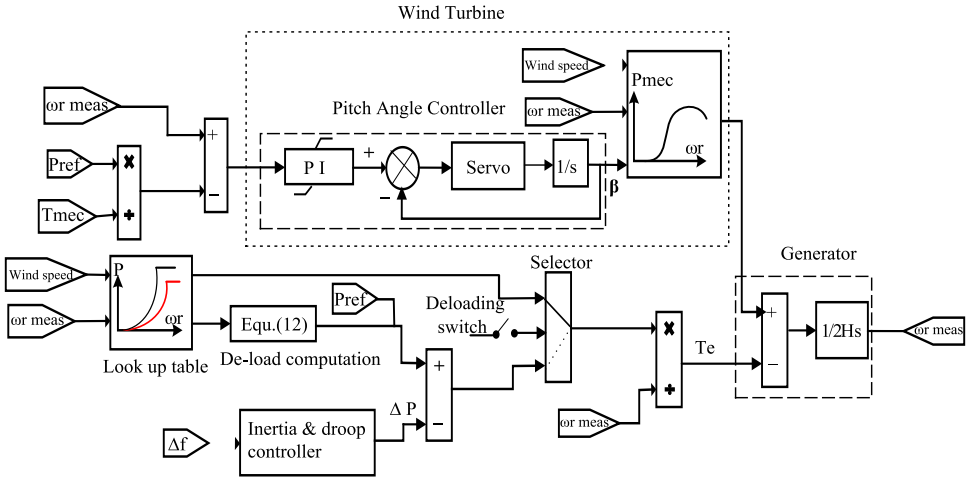


**Fig. 17.** Primary frequency regulation for a DFIG-based wind turbine with de-loading control [47].

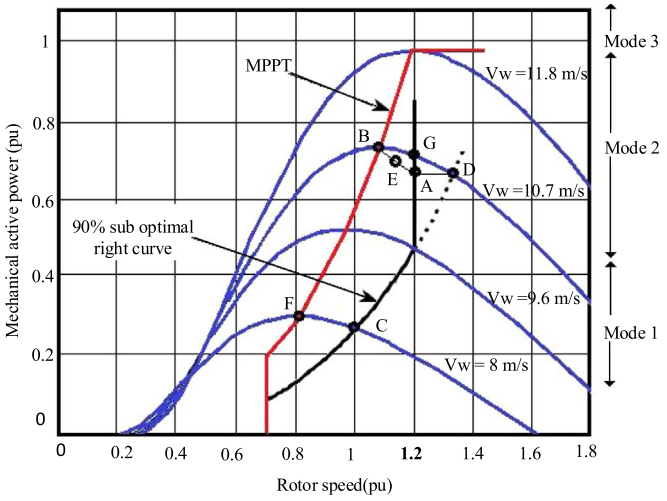


**Fig. 18.** 90% sub-optimal operation curve with the rotor speed limitation [48,49].

variable speed wind turbine is also presented in [18]. This paper proposed three operating modes depending on the range of wind speed. The author proposed a decision algorithm to manage the cooperation between pitch angle and the over-speed controller. This algorithm determines the power set value for the pitch angle controller and the power margin for the over-speed controller.

Another study [50] used cooperation between pitch angle and over-speed controller to allow the wind turbine to participate in frequency regulation. However, this time, the controllers made their decision based on reserve power value depending on the network operator request. In [51], the same frequency regulation controllers used for the DFIG wind turbine were redesigned and implemented in the PMSG to enable this type of wind turbine to contribute to primary frequency control.

In [52,53], the pitch and over-speed controllers, coordinated with droop control, were proposed. These controllers were activated based on wind speed ranges to enable the DFIG-based wind turbine to contribute in frequency regulation. Moreover, the over-speed control strategy using wind speed measure to determine the sub-optimal power based on the deloading tracking curve is saved into the look up table.

### 3.2. Solar photovoltaic array contributions in frequency regulation

Recently, the penetration of solar photovoltaic PV into distribution networks has significantly increased. As a result of this, reserve power from the remaining conventional source unit is insufficient to regulate system frequency under island conditions. Moreover, due to the high cost of solar photovoltaic systems, different MPPT techniques have been introduced to extract the maximum power from this source [54–56]. However, the use of MPPT techniques enable the solar photovoltaic PV to operate without any reserve power. For these reasons, different modifications have been made to the design of controllers used with a PV converter to allow them to effectively participate in frequency regulation.

According to [57], smart photovoltaic inverters do not have the full commercial control capability to change the output power from PV systems, even if they have the ability to provide frequency down-regulation by curtailing power. Moreover, research related to this type of control is still in its early stages, and mainly rely on two types of controller. The first type uses solar photovoltaic PV supported by ESS to regulate frequency; this type will be discussed in Section IV (B.), while the second type proposes the deloading technique for solar photovoltaic PV without ESS, as presented in [58–60]. These papers present a comprehensive control scheme, which allows the photovoltaic system to regulate frequency. Fig. 19 shows the deloading technique, which is achieved by increasing the PV voltage beyond the *MPP voltage*. This is achieved by increasing the value from $V_{MPP}$ by voltage $V_{deload}$, which allows the PV array to maintain some reserve power. This reserve power will not be released until the system frequency deviates. Under these conditions, a control signal proportional to frequency deviation $V_{dc\Delta f}$ is added to the dc reference voltage.

It is clearly shown in Fig. 19 that the change in output power from the PV will not only depend on the $V_{MPP}$ value, but also depends on the frequency deviation, as given by Eq. (13).

$$Vdcref = V_{MPP} + V_{deload} - V_{dc\Delta f} \tag{13}$$

The operation of the deloaded controller is illustrated in Fig. 20, where PV is working at point 3 to maintain some reserve power. This situation continues until the system frequency begins to decline, at which point, a control signal related to frequency deviation will reduce the PV voltage, and make the PV work at point 2.

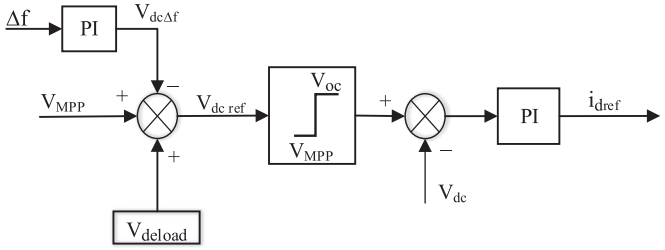


**Fig. 19.** Controller for de-loaded solar PV [60].

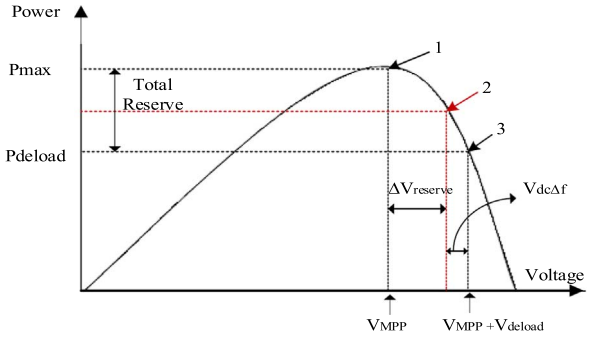


**Fig. 20.** Solar PV with de-loading technique [61].

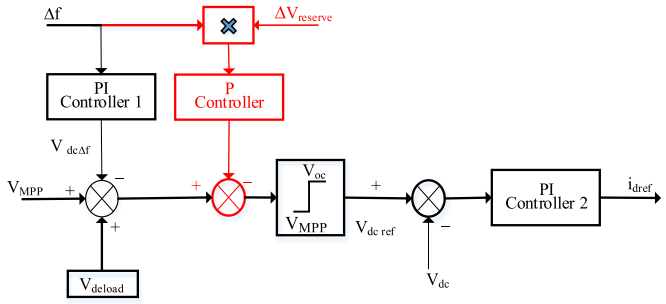


**Fig. 21.** Improved controller for de-loaded PV which considers the amount of available reserve [61].

In fact, the controller discussed in Fig. 19 has a big problem in that it does not take into consideration the remaining reserve power for each PV unit. For this reason, all PV units will release same amounts of active power needed for frequency regulation, even of the reserve power of each unit will not be equal. As a result of this, some PV units with less reserves will reach the MPP faster and will not be able to contribute any further to frequency regulation. This will lead to the non-uniform distribution of frequency regulation. Ref. [61] proposed a new modification to the previous controller by adding a new control signal representing the remaining reserve power $\Delta V_{reserve}$, as shown in Fig. 21. The reference voltage of the new controller is given by Eq. (14), which clearly shows that the output power released from the PV units is not equal, and depends on the reserve power available for each one.

$$Vdcref = (V_{MPP} + V_{deload} - V_{dc\Delta f}) - (\Delta f \times \Delta Vreserve \times K_{P2}) \quad (14)$$

Another technique proposed in [62] enables a solar PV plant to regulate frequency. Two algorithms were implemented; the first was the traditional MPPT controller, which is responsible for operating the PV plant on MPP during normal operations. For transient conditions, a control signal would activate the deloading algorithm, which uses a modified fractional open circuit voltage. This modification proposed the usage of the ratio K as a controlled variable, which determines the amount of reserve power for PV plants limited to the range (0.8–0.95). The main finding of this paper shows that a PV generator has the ability to regulate the frequency and follow load changes. In addition, [63] discussed a control scheme designed for a PV panel to regulate the frequency of an islanded micro-grid. The main objective of this paper was to use a tracking algorithm to follow a command signal, which changes according to the frequency deviation of the micro-grid. Following this, the control system continues until the controller reaches the PMPP, after which the PV panel stays running on the PMPP.

Generally, all control techniques discussed in this paper were designed to provide the solar PV system with reliable control to regulate the frequency in grid connected or off-grid mode. These techniques were mainly based on the MPPT controller running the

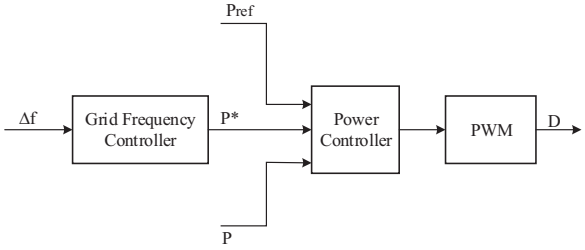


**Fig. 22.** Solar PV frequency regulator.

PV array in the deloading mode. In contrast, [64] proposed a frequency regulator consisting of an adaptive frequency scheme using nonlinear control to calculate the active power signal $P^*$, depending on the frequency deviation, as shown in Fig. 22. This signal is needed to update the reference power $P_{ref}$ used by the power controller to determine the output power of the solar PV by regulating the duty cycle ($D$) of the power converter.

## 4. Control techniques designed for RESs supported by energy storage systems

According to previous sections, different control techniques have been proposed to provide RESs with the ability to regulate system frequency during disturbances. However, these techniques have some issues in terms of reliability, as the nature of the RESs depends on variable factors. Therefore, ESSs are needed to work with variable speed wind turbines or solar photovoltaic PVs to increase the reliability of frequency regulation.

### 4.1. Control techniques used for wind turbines supported by ESSs

In [65], cooperation between frequency control techniques and ESS was proposed for the DFIG wind turbine. This cooperation helps overcome problems of frequency control techniques, such as frequency oscillation and the second frequency drop. In fact, the ESS has two main functions in supporting frequency regulation in all wind speed ranges. In the first function, the ESS provides the active power required for speed recovery to prevent the second frequency drop; while in the second, the ESS is regarded as a backup system for the provision of power during deficits.

In [66], primary frequency control was used in wind power plants to maintain a certain level of power reserve. The wind power plant is supported by flywheel storage to fulfil the power reserve requirements set by the network operator. In steady state conditions, a central controller distributes the power reserve requirement between the wind turbines and the flywheel storage system, as shown in Fig. 23. The power reserve margin x (in pu) is determined depending on the wind speed range, and is given by:

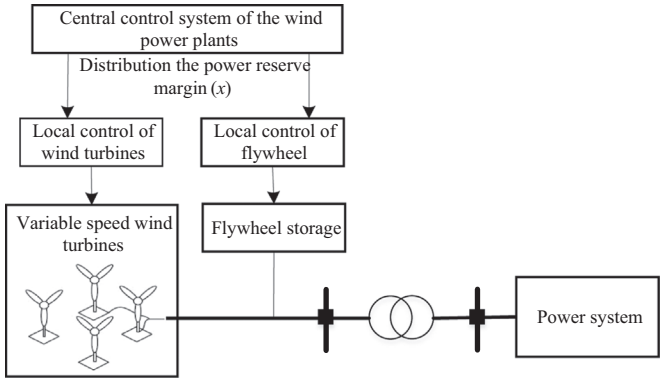


**Fig. 23.** Schematic diagram of frequency regulation of wind turbine and flywheel.

$$1 - x = \begin{cases} \frac{P_{del}}{P_{opt}} \text{if} v_w \leq v_w rated \\ \frac{P_{del}}{P_{rated}} \text{if} v_w > v_w rated \end{cases} \quad (15)$$

where $P_{opt}$ is the maximum power extracted from the wind turbine and $P_{del}$ is the wind turbine power under deloading conditions.

In [67], a virtual inertia technique was proposed for the DFIG wind turbine to provide short-term frequency regulation. Since this technique focuses on short-term oscillation, there is no need for long power regulation. For this reason, a super-capacitor is connected to the DC-link of the DFIG wind turbine inverter via a DC-DC converter. A comparison study done in this work showed that using the DFIG rotating mass or super-capacitor as the virtual inertia source improves system stability. However, each type has different impacts. Although the rotating mass virtual inertia does not require additional components, its performance is highly dependent on fluctuated wind speed. On the other hand, super-capacitor virtual inertia, which can enhance system stability and is independent of wind speed, require new components.

### 4.2. Control techniques used for a solar PV plant supported by an ESS

In [68], the power modulation technique used for PV generation output was described as using a double layer super-capacitor in the manner shown in Fig. 24. This figure shows a PV generation system, consisting of a PV array, an inverter, and a super-capacitor. The array generates dc power $P_S$. After that, the inverter converts the dc power to ac power $P$, and transmits this power to the utility via a service line. The super-capacitor is used to absorb the difference $P_C$ between $P_S$ and $P$.

The proposed frequency controller is shown in Fig. 25. This figure shows that if the frequency deviation is smaller than 0.1 Hz, then the output $P_f$ is given by $G\ (f_{ref}–f)$. However, it is limited to within $\pm P_{mod}$, which is considered 3% of the generation capacity.

A frequency and voltage regulation technique using PV systems and Li-ion batteries coupled to the grid was presented in [69]. This technique allows effective control over the active and reactive power available from the system. This work proposes that the system be allowed to participate in frequency regulation. Down-regulation is where the storage battery absorbs the output power from the PV system and excess power from the grid, while Up-regulation is where the PV/battery system injects active power into the grid. A proposed system, comprising of a 2 kW PV array, 2.64 kW h batteries with bi-directional dc-dc converter, and a three phase inverter and the grid, was modelled and simulated in MATLAB. According to this paper, the PV plant can respond quickly and participate in frequency regulation.

In [70], the Frequency regulation using a PV plant supported by an ESS was presented. This paper proposed a comprehensive control system using P-Q based droop control. This control system automatically regulates the active and reactive power, where the demand power exceeds that generated by PV arrays. However, when the power demanded by the grid is less than the PV array, the inverter control switches to regulate the frequency and voltage based on active and reactive set points. The proposed controller take the decision of frequency regulation based on the output power from PV system and battery state of charge (SOC).

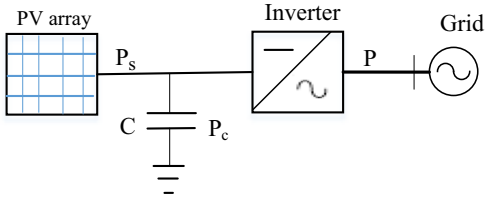


**Fig. 24.** PV and super-capacitor used in frequency regulation.

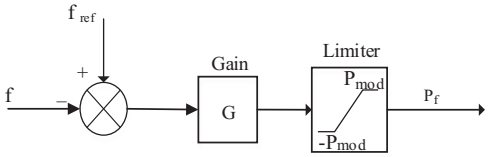


**Fig. 25.** Frequency controller using limiter block [68].

Another research using the same principles of P-Q control for a Microgrid with PV generator and battery storage was presented in [71]. This paper proposed the smooth transition of the PV from P-Q control in the grid connected mode to V-f control in the islanded mode. The proposed transition of solar PV to V-f control demonstrated a very satisfactory performance in restoring voltage and frequency back to nominal values in a matter of only 2 s. The control strategies presented in this paper involve operating the PV generator on MPP supported by battery storage. This battery storage injects and absorb deficit or surplus power using the charge/discharge cycle of the battery.

## 5. Inertia and frequency regulation controllers based on soft computing approaches

In the near future, the complexity/nonlinearity of the power systems will increase due to continuous integration of RESs. For this reason, the classical controller such as proportional-integral (PI) controller will not be suitable for a wide range operation. Therefore, a robust control scheme that use optimal/intelligent techniques are required. Authors in [72] proposes an inertia and frequency regulation controller based on the fuzzy logic control for DFIG wind turbine. As shown in Fig. 26, the fuzzy controller continuously tunes the values of $k_1$, $k_2$, $k_f$ based on frequency deviation $\Delta f$ and wind power deviation $\Delta P_w$. The simulation study shows the importance of the proposed fuzzy controller in making the power system respond dynamically to load changes.

Another research using the same principles of tuning the classical PI controller by soft computing technique was presented in [73]. This paper uses the PSO technique to improve the membership functions of the fuzzy controller, which is used to tune the PI controller constants, as shown in Fig. 27.

A comparison study done in [73] between the classical PI controller, fuzzy tuning approach and PSO-based fuzzy tuning approach shows the robustness of proposed PSO-based fuzzy tuning approach over the other two methods. Another comparison study was done in [74] between classical PID controller and adaptive neural network (ANN) controller to regulate the frequency of isolated network, where this network contains wind and diesel generators without ESS. The simulation study shows the advantages of the proposed ANN in terms of overshoot frequency, undershoot frequency, and settling time.

As discussed in Section 3.1.3, frequency regulation control proposed for the wind turbine is realized using the deloading technique. This technique is used to keep a fixed amount of reserve power to compensate the power shortages. However, keeping a fixed value of reserve power will reduce the annual capacity factor (CF) of wind farms, since the output power from this source is not constant. For this reason, authors in [75] recommend the usage of online deloading technique based on fuzzy logic controller to adjust the deloading factor continuously based on frequency deviation. Furthermore, [76] propose a frequency regulation control for PV generator based on fuzzy logic controller. This controller use frequency deviation and solar radiation as inputs to determine the reference power injected by the PV inverter as shown in Fig. 28. The simulation study proved the effectiveness of proposed method for regulating frequency.

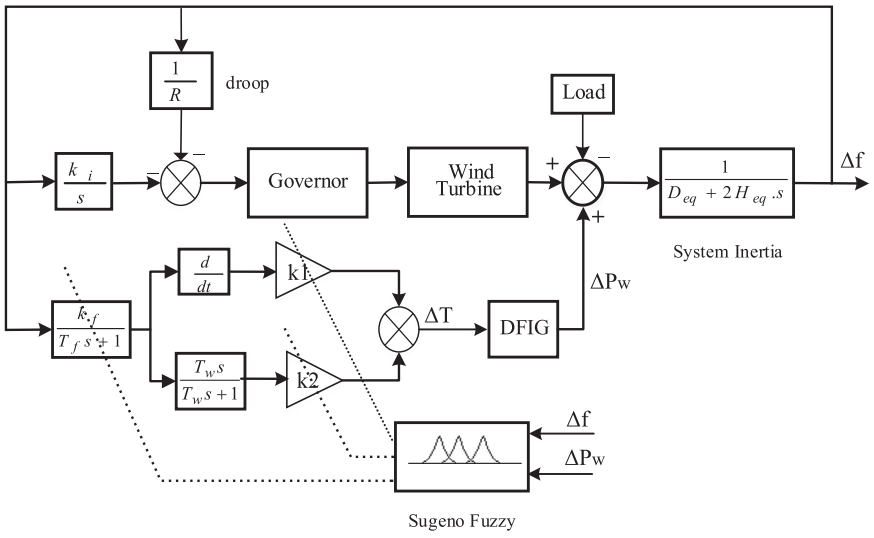


**Fig. 26.** DFIG wind turbine frequency regulation using fuzzy tuning-based PI controller [72].

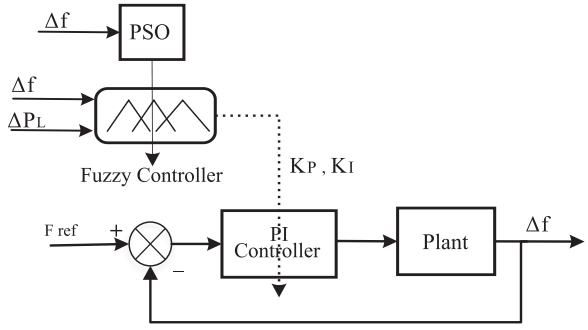


**Fig. 27.** DFIG wind turbine frequency regulation based on PSO and fuzzy controller [73].

## 6. Discussion

This paper discusses several proposed inertia and frequency control techniques for wind turbine and solar PV. Some researchers propose the use of frequency regulation controller without support from ESS, where they succeed in regulating the frequency during supply shortages. On the other hand, other researchers propose an ESS support for frequency regulation over a wide operational range [77]. Due to intermittent RESs and fluctuate power output, it is necessary to use the ESS to raise the reliability of the control system, even if it increase the total cost of power system. Generally, selecting the best frequency regulation technique, whether supported by ESS or not, should depend on the power system requirements. In other words, a balance between the need for reliability and cost of controller technique must be adopted as a basis for selection. The overall advantages and disadvantages of each technique are summarized in the following table. (Table 1).

Integrating a high number of RESs into power systems introduces critical frequency stability issues. For this reason, an inertia and frequency controllers is required to allow the RESs to participate in frequency regulation. However, to simplify the integration of RESs into power systems, some important recommendations should be clearly defined.

A) Define a new grid code and standards: Additional studies should be done to define a new grid code and standards to be suitable for contribution of large-scale RESs. The new grid code should consider the requirements of frequency regulation of RESs.
B) Revising the existing reserve policy: Further studies and economic analysis are needed to determine the proper reserve margin, where the identification of this margin should consider the balance between cost and technical performance.
C) Developing new storage technologies used for frequency regulation: with the increase in the number of RESs connected into grid, the necessity for ESS has been increased. For this reason, additional

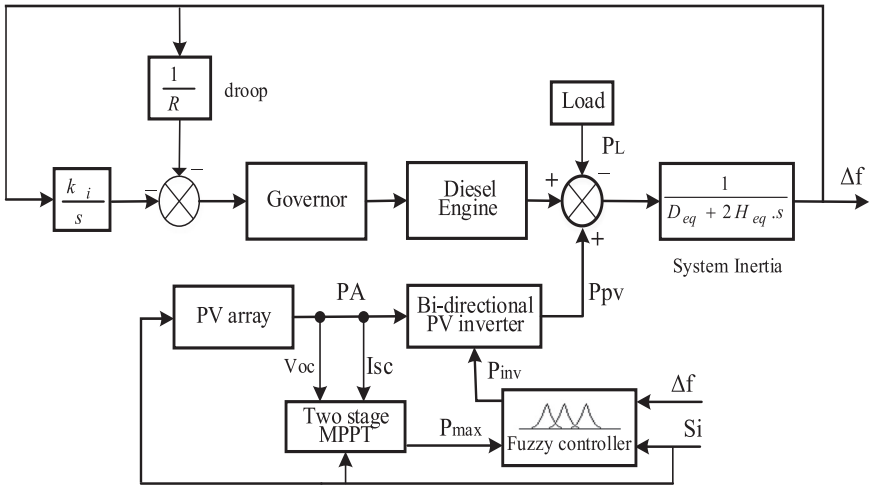


**Fig. 28.** Fuzzy-based frequency regulation control for PV diesel system [76].

**Table 1**
Advantages and disadvantages of inertia and frequency control techniques for RESs.

| ESS | Type of source | Techniques | Advantages | Disadvantages |
|---|---|---|---|---|
| No | Solar PV plant | Deloading Technique | Does not need additional component | Loses a certain percentage of energy |
| | | | Can provide inertial and frequency control | Depends on environmental conditions |
| | Variable speed wind turbine | Inertial Response Technique | Power extracted directly from rotating mass | Second frequency drop may be happened |
| | | Deloading Technique | Provides primary frequency control | Loses a certain percentage of energy |
| Yes | Solar PV plant | Deloading | Highly reliable system | High cost due to battery price and loses a certain energy |
| | | MPPT | Eliminates the power fluctuations | Fails to absorb power from grid if the battery is fully charged |
| | Variable speed wind turbine | Inertial response Deloading | Prevents second frequency drop Highly reliable technique | High cost due to battery price and some energy |

study should be done to find cheap and effective storage systems such as hydro pumping storage, superconducting magnetic energy storage, and electrical vehicle storage [78].

## 7. Conclusions and future research

In the near future, power systems networks will experience a significant increase in the penetration level of RESs. For example, by 2020, renewable capacity will be enough to supply an estimated 26% of global electricity needs [79]. However, integrating more RESs into power systems will reduce the number of conventional generation units that provide primary frequency control and inertia response. For example, the inertia response of NORDIC power system will be reduced by 35% between 2010 and 2020 [80]. For this reason, a new control scheme must be integrated with RESs to provide inertia and primary frequency control. This paper reviewed several inertia and frequency regulation controllers for wind turbine and solar photovoltaic plants with and without ESS. Whether supported by ESS or not, the inertia and frequency regulation controller discussed in this work is suitable for the present penetration level of RESs. However, for future power system with high penetration level of RESs, further studies must be conducted to develop an effective, intelligent, and robust primary frequency regulation schemes. A coordination between the primary frequency control and frequency protection controller, such as load shedding controller, will be required. Furthermore, advanced computing methods and fast communication technologies will be needed to realize the adaptive frequency control scheme.

## Acknowledgement

The authors would like to thank the Ministry of Higher Education of Malaysia for providing financial support under the research Grant NO: HIR-MOHE D000004-16001).

## References

[1] Dong J, Xue G, Dong M, Xu X. Energy-saving power generation dispatching in China: regulations, pilot projects and policy recommendations—a review. Renew Sustain Energy Rev 2015;43:1285–300.
[2] Saidur R, Rahim N, Islam M, Solangi K. Environmental impact of wind energy. Renew Sustain Energy Rev 2011;15:2423–30.
[3] Kyoto Protocol to the United Nations framework convention on climate change. Available online at: ⟨http://unfccc.int/resource/docs/convkp/kpeng.pdf⟩; 1997 [accessed 01.10.15]
[4] Cleaner and Cheaper: Using the clean air act to sharply reduce carbon pollution from existing power plants, delivering health, environmental, and economic benefits. Available online at: ⟨https://www.nrdc.org/file/3410/download?token=6c64p-xd⟩; 2014 [accessed 18.03.15]
[5] Renewable EnergyTarget Scheme. Available online at: ⟨http://www.aph.gov.au/DocumentStore.ashx?id=17008e4b-e2f3-4ea3-9d53-fb3fb0cd4d85 & subId=351098⟩; 2014 [accessed 17.11.15]
[6] Renewables Global Status Report, REN21.Available online at: ⟨http://www.ren21.net/Portals/0/documents/Resources/GSR2012_low%20res_FINAL.pdf⟩; 2012 [accessed 01.05.15].
[7] Mahzarnia M, Sheikholeslami A, Adabi J. A voltage stabilizer for a microgrid system with two types of distributed generation resources. IIUM Eng J 2013:14.
[8] Chun Su. Line Effects of distribution system operations on voltage profiles in distribution grids connected wind power generation. Proc IEEE Power Syst Technol 2006:1–7.
[9] Ausavanop O, Chaitusaney S. Coordination of dispatchable distributed generation and voltage control devices for improving voltage profile by Tabu Search. In: Proc IEEE Elec Eng/Elect, Comp, Telecommun and Inform Technol Conf (ECTI-CON); 2011. p. 869–72.
[10] Sekhar ASR, Vamsi Krishna K. Improvement of voltage profile of the hybrid power system connected to the grid. Int J Eng Res Appl 2012;2:87–93.
[11] Bevrani H, Ghosh A, Ledwich G. Renewable energy sources and frequency regulation: survey and new perspectives. Renew Power Generation, IET 2010; 4: p. 438–57.
[12] Dehghanpour K, Afsharnia S. Electrical demand side contribution to frequency control in power systems: a review on technical aspects. Renew Sustain Energy Rev 2015;41:1267–76.
[13] Electricity Ten Year Statement (ETYS). Available online at ⟨http://www2.nationalgrid.com/UK/Industry-information/Future-of-Energy/Electricity-ten-year statement /⟩; 2014 [accessed 11.05.15]
[14 UK Future Energy Scenarios.Available online at ⟨http://www2.nationalgrid.com/WorkArea/DownloadAsset.aspx?Id=10451⟩; 2013 [accessed 11.05.15]
[15] Jayawardena A., Meegahapola L., Perera S., Robinson D. Dynamic characteristics of a hybrid microgrid with inverter and non-inverter interfaced renewable energy sources: a case study. In: Proceedings of IEEE Power Syst Techno (POWERCON); 2012. p. 1–6.
[16] Ulbig A, Borsche TS, Andersson G. Impact of low rotational inertia on power system stability and operation. arXiv preprint arXiv:1312.6435; 2013.
[17] Kundur P, Balu NJ, Lauby MG. Power system stability and control. New York: McGraw-hill; 1994.
[18] Díaz-González F, Hau M, Sumper A, Gomis-Bellmunt O. Participation of wind power plants in system frequency control: review of grid code requirements and control methods. Renew Sustain Energy Rev 2014;34:551–64.
[19] Machowski J, Bialek J, Bumby J. Power system dynamics: stability and control, 2nd Edition. John Wiley & Sons; 2011, ISBN: 978-1-84628-492-2 (Print) 978-1-84628-493-9 (Online).
[20] Yu M, Dysko A, Booth CD, Roscoe AJ, Zhu J. A Review of Control Methods for providing frequency response in VSC-HVDC transmission systems. In: Proceedings of IEEE Power Eng Conf (UPEC); 2014. p. 1–6.
[21] Gonzalez-Longatt F.M. Effects of the synthetic inertia from wind power on the total system inertia: simulation study. In: Proceedings of IEEE environment friendly energies and appl conference (EFEA); 2012. p. 389–95.
[22] Rebours YG, Kirschen DS, Trotignon M, Rossignol S. A survey of frequency and voltage control ancillary services—Part I: Technical features. IEEE Trans Power Syst 2007;22:350–7.
[23] Thresher R, Robinson M, Veers P. To capture the wind. IEEE Power Energy Mag 2007;5:34–46.
[24] Mauricio JM, Marano A, Gómez-Expósito A, Martinez Ramos JL. Frequency regulation contribution through variable-speed wind energy conversion systems. IEEE Trans Power Syst 2009;24:173–80.
[25] Revel G, Leon AE, Alonso DM, Moiola JL. Dynamics and stability analysis of a power system with a PMSG-based wind farm performing ancillary services. IEEE Trans Circuits Syst I 2014;61(7):2182–93.
[26] Bianchi FD, De Battista H, Mantz RJ. Wind turbine control systems: principles, modelling and gain scheduling design. Springer Science & Business Media; 2006, ISBN: 978-1-84628-492-2.
[27] Singh B, Sharmay S. Stand-alone wind energy conversion system with an asynchronous generator. J Power Electr 2010;10:538–47.
[28] Lamchich MT, Lachguer N. Matlab simulink as simulation tool for wind generation systems based on doubly fed induction machines. INTECH Open Access Publisher; 2012.
[29] Knudsen H, Nielsen JN. Introduction to the modelling of wind turbines. Wind Power in Power Systems, Second Edition:767-97; 2005.
[30] Sun Y-z, Zhang Z-s, Li G-j, Lin J. Review on frequency control of power systems with wind power penetration. In: Proceedings of IEEE Power Syst Technol Conference (POWERCON), 2010. p. 1-8.
[31] Ekanayake J, Jenkins N. Comparison of the response of doubly fed and fixed-speed induction generator wind turbines to changes in network frequency. IEEE Trans Power Syst Energy Convers 2004;19:800–2.
[32] Gonzalez-Longatt F., Chikuni E., Rashayi E. Effects of the synthetic inertia from wind power on the total system inertia after a frequency disturbance. In: Proceedings of IEEE Ind Technol Conference (ICIT); 2013. p. 826–32.
[33] Morren J, Pierik J, De Haan SW. Inertial response of variable speed wind turbines. Electr Power Syst Res 2006;76:980–7.

[34] Wu L, Infield DG. Towards an assessment of power system frequency support from wind plant—modeling aggregate inertial response. IEEE Trans Power Syst 2013;28:2283–91.
[35] Morren J, De Haan SW, Kling WL, Ferreira J. Wind turbines emulating inertia and supporting primary frequency control. IEEE Trans Power Syst 2006;21:433–4.
[36] Zhang Z., Wang Y., Li H., Su X. Comparison of inertia control methods for DFIG-based wind turbines. in: Proceedings of IEEE ECCE Asia Downunder (ECCE Asia); 2013. p. 960–4.
[37] Wachtel S, Beekmann A. Contribution of wind energy converters with inertia emulation to frequency control and frequency stability in power systems.In: Proceedings of the 8th international workshop on large scale integration of wind power into power systems as well as on offshore wind farms, Bremen, Germany; 2009.
[38] Ullah NR, Thiringer T, Karlsson D. Temporary primary frequency control support by variable speed wind turbines—potential and applications. IEEE Trans Power Syst 2008;23:601–12.
[39] Hansen AD, Altin M, Margaris ID, Iov F, Tarnowski GC. Analysis of the short-term overproduction capability of variable speed wind turbines. Renew Energy 2014;68:326–36.
[40] El Itani S., Annakkage U.D., Joos G. Short-term frequency support utilizing inertial response of DFIG wind turbines. In: Proceedings of IEEE power and energy soc general meeting; 2011. p. 1–8.
[41] Keung P-K, Li P, Banakar H, Ooi BT. Kinetic energy of wind-turbine generators for system frequency support. IEEE Power Syst 2009;24:279–87.
[42] Mishra S., Zarina P., Sekhar P. A novel controller for frequency regulation in a hybrid system with high PV penetration. In: Proceedings of IEEE Power and Energy Soc General Meeting (PES); 2013. p. 1–5.
[43] Josephine R, Suja S. Estimating PMSG wind turbines by inertia and droop control schemes with intelligent fuzzy controller in Indian. Dev J Elect Eng Technol 2014;9:1196–201.
[44] Yao W., Lee K.Y. A control configuration of wind farm for load-following and frequency support by considering the inertia issue. In: Proceedings of IEEE Power and Energy Soc General Meeting; 2011. p. 1–6.
[45] Eid BM, Rahim NA, Selvaraj J, El Khateb AH. Control methods and objectives for electronically coupled distributed energy resources in microgrids:a review. IEEE Syst J 2014:1–13.
[46] Castro LM, Fuerte-Esquivel CR, Tovar-Hernández JH. Solution of power flow with automatic load-frequency control devices including wind farms. IEEE Trans Power Syst 2012;27:2186–95.
[47] Vidyanandan K, Senroy N. Primary frequency regulation by deloaded wind turbines using variable droop. IEEE Trans Power Syst 2013;28:837–46.
[48] Zhang Z-S, Sun Y-Z, Lin J, Li G-J. Coordinated frequency regulation by doubly fed induction generator-based wind power plants. IET Renew Power Gener 2012;6:38–47.
[49] Ramtharan G, Jenkins N, Ekanayake J. Frequency support from doubly fed induction generator wind turbines. IET Renew Power Gener 2007;1:3–9.
[50] De Almeida RG, Peas Lopes J. Participation of doubly fed induction wind generators in system frequency regulation. IEEE Trans Power Syst 2007;22:944–50.
[51] Wu Z, Gao W, Wang J, Gu S. A coordinated primary frequency regulation from permanent magnet synchronous wind turbine generation. In: Proceedings of IEEE Power Electron and Mach in Wind Appl Conf (PEMWA); 2012. p. 1–6.
[52] Zhangjie C, Xiaoru W, Jin T. Control strategy of large-scale DFIG-based wind farm for power grid frequency regulation. In: IEEE Control Conference (CCC) 2012 31st Chinese; 2012. p. 6835–40.
[53] Tielens P, De Rijcke S, Srivastava K, Reza M, Marinopoulos A, Driesen J. Frequency support by wind power plants in isolated grids with varying generation mix. In: Proceedings of IEEE Power and Energy Soc General Meeting; 2012. p. 1–8.
[54] Faranda R, Leva S. Energy comparison of MPPT techniques for PV systems. WSEAS Trans Power Syst 2008;3:446–55.
[55] De Brito MAG, Galotto L, Sampaio LP, de Azevedo e Melo G, Canesin CA. Evaluation of the main MPPT techniques for photovoltaic applications. In: Proceedings of IEEE Trans Ind Electron. 2013; 60: p. 1156–67.
[56] Hua C, Shen C Study of maximum power tracking techniques and control of DC/DC converters for photovoltaic power system. In: Proceedings of IEEE Power Electron Specialists Conference, 1998 PESC 98 Record 29th Annual IEEE; 1998. p. 86–93.
[57] Hoke A., Maksimovic D. Active power control of photovoltaic power systems. In: Proceedings of the 1st IEEE Conference IEEE Technol for Sustainability (SusTech) Conference, 2013; 2013. p. 70–7.
[58] Zarina P, Mishra S, Sekhar P. Deriving inertial response from a non-inertial PV system for frequency regulation. In: Proc IEEE Int Drives and Energy Syst Conf (PEDES) on IEEE Power Electronics; 2012. p. 1–5.
[59] Rahmann C, Castillo A. Fast frequency response capability of photovoltaic power plants: the necessity of new grid requirements and definitions. Energies 2014;7:6306–22.
[60] Zarina P, Mishra S, Sekhar P Photovoltaic system based transient mitigation and frequency regulation. In: Proceedings of the 2012 Annual IEEE India Conference (INDICON); 2012. p. 1245–9.
[61] Zarina P, Mishra S, Sekhar P. Exploring frequency control capability of a PV system in a hybrid PV-rotating machine-without storage system. Int J Elect Power Energy Syst 2014;60:258–67.
[62] Pappu VAK, Chowdhury B, Bhatt R. Implementing frequency regulation capability in a solar photovoltaic power plant. In: Proceedings of North Amer Power Symp Conf (NAPS); 2010. p. 1–6.
[63] Watson LD, Kimball JW. Frequency regulation of a microgrid using solar power. In: Proceedings of IEEE Appl Power Electron Conf and Exposition (APEC); 2011. p. 321–6.
[64] Okou A, Akhrif O, Beguenane R, Tarbouchi M Nonlinear control strategy insuring contribution of PV generator to voltage and frequency regulation. In: Proceedings of the 6th IET International Conference on Power Electron, Mach and Drives (PEMD 2012). IET; 2012. p. 1–5.
[65] Miao L., Wen J., Xie H., Yue C., Lee W.-J. Coordinated control strategy of wind turbine generator and energy storage equipment for frequency support. Ind Appl Soc Annu Meeting; 2014. p. 1–7.
[66] Díaz-González F, Hau M, Sumper A, Gomis-Bellmunt O. Coordinated operation of wind turbines and flywheel storage for primary frequency control support. Int J Elect Power Energy Syst 2015;68:313–26.
[67] Arani MFM, El-Saadany EF. Implementing virtual inertia in DFIG-based wind power generation. IEEE Trans Power Syst 2013;28:1373–84.
[68] Kakimoto N, Takayama S, Satoh H, Nakamura K. Power modulation of photovoltaic generator for frequency control of power system. IEEE Trans Energy Convers 2009;24:943–9.
[69] Bhatt R, Chowdhury B. Grid frequency and voltage support using PV systems with energy storage. In: Proceedings of North Amer Power Symp Conf (NAPS); 2011. p. 1–6.
[70] Chamana M, Chowdhury BH. Droop-based control in a photovoltaic-centric microgrid with Battery Energy Storage. In: Proceedings of North Amer Power Symp Conf (NAPS); 2013. p. 1–6.
[71] Adhikari S, Li F. Coordinated Vf and PQ control of solar photovoltaic generators with MPPT and battery storage in microgrids. IEEE Trans Smart Grid 2014;5:1270–81.
[72] Sa-ngawong N, Ngamroo I. Optimal fuzzy logic-based adaptive controller equipped with DFIG wind turbine for frequency control in stand alone power system. In: Proceedings of the 2013 IEEE Innovative Smart Grid Technologies-Asia (ISGT Asia); 2013 Nov 10. p. 1–6.
[73] Bevrani H, Habibi F, Babahajyani P, Watanabe M, Mitani Y. Intelligent frequency control in an ac microgrid: online PSO-based fuzzy tuning approach. IEEE Trans Smart Grid 2012;3(4):1935–44.
[74] Ali SQ, Hasanien HM. Frequency control of isolated network with wind and diesel generators by using adaptive artificial neural network controller. International Review of Automatic Control I. RE. A. CO;5; 2012.
[75] Pradhan C, Bhende CN. Adaptive deloading of stand-alone wind farm for primary frequency control. Energy Syst 2015;6(1):109–27.
[76] Datta M, Senjyu T, Yona A, Funabashi T, Kim CH. A frequency-control approach by photovoltaic generator in a PV–diesel hybrid power system. IEEE Trans Energy Convers 2011;26(2):559–71.
[77] Rodrigues E, Osório G, Godina R, Bizuayehu A, Lujano-Rojas J, Catalão J. Grid code reinforcements for deeper renewable generation in insular energy systems. Renew Sustain Energy Rev 2016;53:163–77.
[78] Tan KM, Ramachandaramurthy VK, Yong JY. Integration of electric vehicles in smart grid: a review on vehicle to grid technologies and optimization techniques. Renew Sustain Energy Rev 2016;53:720–32.
[79] Renewable Energy Medium-Term Market Report. Available online at: ⟨https://www.iea.org/Textbase/npsum/MTrenew2015sum.pdf⟩; 2015 [accessed 05.07.16]
[80] Future system inertia report. European network of transmission system operators for electricity. Available online at: ⟨https://www.entsoe.eu/Documents/Publications/SOC/Nordic/Nordic_report_Future_System_Inertia.pdf⟩; 2013 [accessed 05.07.16]